The Microwave Spectrum of Silylisothiocyanate, SiH_3NCS

II. r_s-Structure, Dipolmoment and ^{14}N-quadrupole Coupling Constant. A Contribution to the Study of the SiN-bond

K.-F. Dössel and D. H. Sutter

Abteilung für Chemische Physik im Institut für Physikalische Chemie
der Christian Albrechts Universität, Kiel, Germany

(Z. Naturforsch. **32 a**, 473–481 [1977]; received February 16, 1977)

The microwave spectra of ^{15}N- and ^{13}C-substituted SiH_3NCS were recorded in the frequency region between 8 and 40 GHz. Combining the resulting rotational constants with values obtained previously for other isotopic species, the complete r_s-structure of the heavy atom chain could be determined. This leads to the following r_s-bond distances: $r_{C-S} = 1.574_5$ Å, $r_{N-C} = 1.220_8$ Å, and $r_{Si-N} = 1.672_5$ Å. From Stark effect splittings the electric dipole moment of the most abundant species was determined for the ground vibrational state and for the first excited state of the lowest frequency bending vibration v_{10}. The values are $\langle v_{10}=0 \mid \mu_z \mid v_{10}=0\rangle = 2.38 \pm 0.02$ D and $\langle v_{10}=1, l=1 \mid \mu_z \mid v_{10}=1, l=1\rangle = 2.36 \pm 0.02$ D. The direction of the dipole moment is discussed. From the quadrupole hyperfinestructure of the $J=2 \rightarrow J'=3$ rotational transition the ^{14}N-quadrupole coupling constant could be determined as $\chi_{zz}=0.75$ MHz. The experimental results are compared to CNDO/2 calculations.

Introduction

Silylisothiocyanate provides an interesting example for the study of the SiN-bond. As is known since the work of Kewley et al. [1, 2] the molecule is a symmetric top with a linear arrangement of the heavy atom chain. This result may appear surprising at first sight, since the simple nonpolar valence formula (I) with an sp^2 hybridized nitrogen atom would imply a bent structure. (Such a bent structure has indeed been found for the related molecule HNCS with a bond-angle $\sphericalangle H-N-C = 135^\circ$ [3].)

(I) (II)

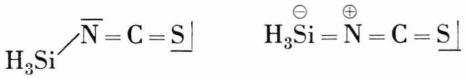

(III)

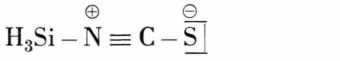

It is however possible to draw two more valence formulae (II) and (III), both highly polar, which would favour the observed linear arrangement of the Si–N–C–S-chain. Since the limiting mesomer forms (II) and (III) would lead to different bond distances and to opposite polarities of the molecular electric dipole moment, it was desirable to determine a complete r_s-structure [4] of the Si–N–C–S-chain together with the electric dipole moment. We therefore analyzed the microwave rotational spectra of two more isotopes, $H_3{}^{28}Si^{15}N^{12}C^{32}S$ and $H_3{}^{28}Si^{14}N^{13}C^{32}S$, yielding accurate rotational constants B_0 and centrifugal distortion constants D_J and D_{JK} for both isotopes. Furthermore vibronic expectation values for the z-component of the molecular electric dipole moment were determined for the vibrational ground state and for the first excited state of the degenerate bending vibration ν_{10}. (The z-axis points into the direction of the molecular symmetry axis.) In addition we have analyzed the ^{14}N nuclear quadrupole hyperfine structure of the rotational transitions, which provides information on the immediate electronic environment of the ^{14}N nucleus. A discussion of the experimental results, including a comparison with the results of CNDO-calculations [5] is given at the end of this paper.

Reprint requests to Prof. D. H. Sutter, Institut für Physikalische Chemie, Christian Albrechts Universität, Olshausenstrasse 40–60, *D-2300 Kiel*, Germany.

Experimental

The samples were prepared by streaming $H_3{}^{28}SiBr$-vapour through tubes packed with $Ag^{32}S^{12}C^{15}N$ and $Ag^{32}S^{13}C^{14}N$ resp. The latter compounds we prepared by smelting $K^{12}C^{15}N$ ($K^{13}C^{14}N$) with sulfur, taking up the melt in dilute H_2SO_4 and precipitating $Ag^{32}S^{12}C^{15}N$ ($Ag^{32}S^{13}C^{15}N$) by addition of $AgNO_3$.

Since H_3SiNCS readily reacts with water, rests of water adsorbed to the walls of the waveguide absorption cell had to be removed by pumping the cell at $+90\,^\circ C$ for several days. The spectra were recorded with a microwave spectrometer of the Hughes-Wilson type [6] described previously [7, 8]. Phase stabi-

lized BWO's as radiation sources and 33 kHz square wave Stark effect modulation were used throughout. Double width X-band absorption cells [9] were used to provide a sufficiently uniform Stark-field over the absorption volume. Typical recording conditions were: sample pressures about 5 mTorr and cell temperatures about $-65\,^{\circ}C$. For the dipole moment determinations involving first order Stark-effects, the standard Square wave generator [10] was replaced by a function generator (Hp 8005A) in order to provide high quality zero based squares below 10 V, peak to peak.

For the vibrational ground state the energy levels of the effective rotational Hamiltonian may be approximated as [11]:

$$W_{JK} = h[B_0(J(J+1) - K^2) + A K^2 - D_K K^4 - D_J J^2(J+1)^2 - D_{JK} J(J+1) K^2] + W_{HFS}. \quad (1)$$

In Eq. (1) B_0 is the effective rotational constant for the ground vibrational state. D_K, D_J and D_{JK} are small centrifugal distortion constants. J and K are the quantum numbers for the square of the overall angular momentum, $\langle P^2 \rangle = \hbar J(J+1)$, and the component of the angular momentum in direction of the molecular symmetry axis, $\langle P_z \rangle = \hbar K$. W_{HFS} stands for the ^{14}N nuclear quadrupole hyperfine contribution. In Silylisothiocyanate it is rather small and may be neglected for higher J transitions (see below).

Since there is no electric dipole moment component perpendicular to the molecular symmetry axis in the vibrational ground state, the electric field vector of the incident microwave radiation has no lever to produce a torque about the figure axis and K is left constant during transitions. For J quantum mechanics leads to the electric field dipole selection rule $\Delta J = \pm 1$. Thus neglecting the ^{14}N hyperfine contribution for a moment Eq. (1) leads to the following frequency expression which was used to fit B_0, D_J and D_{JK} to the observed spectra by a least squares procedure.

$$\nu_{J,K \to J+1,K} = 2B_0(J+1) - 4D_J(J+1)^3 - 2D_{JK}(J+1)K^2. \quad (2)$$

Since D_J is very small in both molecules, high J transitions listed in Tab. 1 were used to determine it accurately. In Tab. 2 the resulting rotational constants and centrifugal constants are given for both molecules. From these the lower J transitions are reproduced within a few kHz, i. e. within the experi-

Table 1. Microwave spectra of ^{13}C and ^{15}N substituted Silylisothiocyanate. The observed frequencies (MHz) are compared to the values calculated from the molecular constants listed in Table 2 according to Equation (2).

$SiH_3N^{13}CS$ $J \to J'$	$8 \to 9$		$9 \to 10$		$10 \to 11$		$11 \to 12$	
K	obs	o−c	obs	o−c	obs	o−c	obs	o−c
0	27254.83	0.00	30283.09	0.00	33311.35	0.03	36339.54	0.00
1	27254.10	0.02	30282.27	0.02	33310.48	0.07	36338.54	0.00
2	27251.82	0.00	30279.70	−0.04	33307.63	−0.01	36335.47	−0.06
3	27248.08	0.02	30275.57	0.00	33303.03	−0.02	36330.51	−0.01
4	27242.79	0.00	30269.66	−0.06	33296.66	0.04	36323.48	−0.02
5	27236.03	0.00	30262.19	−0.01	33288.28	−0.08	36314.48	0.00
6	27227.73	−0.03	30252.94	−0.07	33278.23	−0.01	36303.45	−0.01
7	27217.97	−0.02	—		33266.33	0.02	36290.44	0.00
8	—		30229.59	−0.04	33252.52	0.00	36275.41	0.01
9	—		30215.47	0.04	33236.91	0.00	36258.36	0.00

$SiH_3{}^{15}NCS$ $J \to J'$	$8 \to 9$		$9 \to 10$		$10 \to 11$		$11 \to 12$	
K	obs	o−c	obs	o−c	obs	o−c	obs	o−c
0	—		30290.72	0.01	—		—	
1	—		30289.89	0.03	33318.73	−0.04	—	
2	27258.67	0.03	30287.31	−0.01	33315.95	−0.02	36344.53	−0.08
3	27254.84	0.01	30283.07	−0.01	33311.34	0.02	36339.51	−0.02
4	27249.48	−0.02	30277.16	0.00	33304.79	−0.01	36332.44	0.02
5	27242.66	0.02	30269.52	−0.02	33296.48	0.06	36323.32	0.04
6	27234.26	−0.01	30260.25	0.02	33286.12	−0.06	36312.10	−0.01
7	27224.35	−0.01	30249.23	−0.01	33274.06	−0.02	—	
8	—		—		33260.15	0.02	—	
9	—		—		33244.32	0.00	—	

Table 2. Rotational constants and centrifugal distortion constants of silylisothicyanate. The values for the ^{13}C- and ^{15}N-isotopic species result from a least squares fit to the spectra listed in Table 1. The values for the most abundant species are taken from the work of Dössel and Robiette [12].

Isotopic species	B_0/MHz	D_{JK}/kHz	D_J/kHz
$^{28}SiH_3{}^{14}N^{12}C^{32}S$	1516.040(1)	41.958(6)	0.087(4)
$^{28}SiH_3{}^{15}N^{12}C^{32}S$	1514.552(1)	42.30(1)	0.086(6)
$^{28}SiH_3{}^{14}N^{13}C^{32}S$	1514.169(1)	41.76(1)	0.074(6)

(Numbers in brackets give one standard deviation in units of the last significant figure.)

mental uncertainty. Also listed in Tab. 2 are the corresponding values for the most abundant species [12] which are needed for the r_s-structure determination.

The r_s-Structure of the Si—N—C—S Chain

From the differences in the B_0-values for the ^{15}N- and ^{13}C-isotopes with respect to the B_0 value of the most abundant species it is possible to determine the center of mass distances of the substituted atoms (referred to the center of mass of the most abundant species) via

$$r_s = \sqrt{(I'_\perp - I_\perp)/m}\,. \qquad (3)\ [13]$$

In Eq. (3) the symbols have the following meaning:

$I_\perp = h/8\,r^2\,B_0$ is the molecular moment of inertia about the principal inertia axis perpendicular to the symmetry axis. The prime indicates the substituted species.

$m = [M\,\Delta M/(M+\Delta M)]$ with M = molecular mass of the unsubstituted species and $\Delta M = M' - M$ the change of the molecular mass upon substitution.

Equation (3) follows from the rigid rotor model with atomic masses located at the positions of the nuclei. Since only the difference of the effective moments of inertia enters into the expression, vibrational effects cancel largely and the deviations of the r_s-values from the equilibrium values, r_e, are usually below 0.005 Å [13].

With the B_0 values given in Tab. 2 the Eq. (3) leads to the following center of mass distances for nitrogen and carbon respectively:

$$r_{s(N)} = 0.5764(2)\,\text{Å}, \qquad r_{s(C)} = 0.6444(2)\,\text{Å}.$$

The numbers in bracketts give one standard deviation calculated from the experimental uncertainties in the B_0 values i. e. they do not include esti-

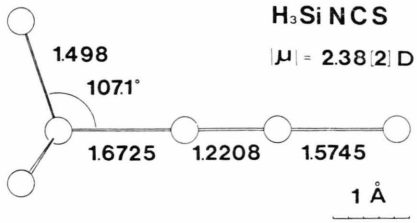

Fig. 1. Absolute value of the electric dipole moment, $|\mu'|$ and r_s-structure of silyl-isothiocyanate. The experimental uncertainties of the r_s-bond-distances are below $5\cdot10^{-4}$ Å. Since vibrational effects tend to cancel in the equations used for the r_s-structure determination, the r_s-bond-distances are believed to come close to the equilibrium distances with typical deviations between r_s- and r_e-values on the order of $5\cdot10^{-3}$ Å [13].

mates on possible vibrational effects causing deviations of the r_s values from the corresponding equilibrium values! Now using the r_s-distances determined by Dössel and Robiette for silicon and sulfur, all bond distances in the Si – N – C – S-chain can be calculated. The resulting complete r_s-structure is given in Fig. 1 where the data for the Silyl-group are taken from the work of Kewley et al. [2].

The Molecular Electric Dipole Moment

The absolute value of the vibrational ground state expectation value of the molecular electric dipole moment was determined from the first order

Table 3. Vibrational ground state Stark satellites for the $K=3$, $J=3\rightarrow J'=4$ and $K=0$, $J=2\rightarrow J'=3$ rotational transitions of the most abundant isotopic species.

Rotational transition $K=3$, $J=3\rightarrow J'=4$			Rotational transition $K=0$, $J=2\rightarrow J'=3$		
Electric field [V/cm]	M_J	Stark-shift [MHz]	Electric field [V/cm]	M_J	Stark-shift [MHz]
31.67	3	11.34	438.2	0	−2.36
31.76	−2	− 7.56	487.3	0	−2.87
31.76	−3	−11.37	591.3	0	−4.20
42.34	2	10.15	684.4	0	−5.57
42.34	1	5.05	781.4	0	−7.39
42.34	−1	− 5.05	848.1	0	−8.79
42.34	−2	−10.15	340.4	2	2.62
52.93	2	12.67	388.9	2	3.43
52.93	−2	−12.63	440.8	2	4.43
63.87	2	15.27	487.3	2	5.35
63.87	−1	− 7.64			
63.83	−2	−15.32			
74.12	−1	− 8.88			
74.12	−2	−17.78			
84.70	−1	−10.09			
84.70	−2	−20.15			

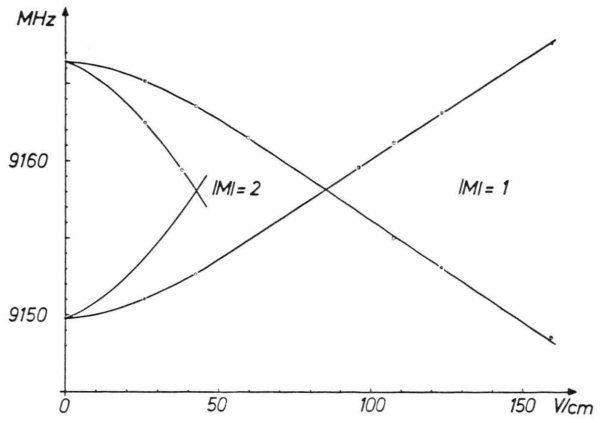

Fig. 2. Frequency versus Stark field plot of the Stark-effect satellites of the $|K|=1$, $J=2\rightarrow J'=3$ l-type doublet in the first excited state of the degenerate bending vibration v_{10}. As is seen from the Fig. satellites with equal $|M|$-values cross at typical Stark-fields $E_c(M)$ at the center gap frequency of the zero field doublet. The crossing field for the $|M|=1$ satellites, $E_c(M=1)=84.2(5)$ V/cm, was used to calculate the vibrational average for $|\mu_z|$ in the first excited state, $v_{10}=1$. The zero field l-doublet splitting is 16.665(20) MHz.

Stark-effect of the $|K|=3$, $J=3\rightarrow J'=4$ transition and from the second order Stark-effect of the $K=0$, $J=2\rightarrow J'=3$ transition of the most abundant isotopic species (see Table 3). The spectrometer was calibrated using OCS with $\langle 0|\mu|0\rangle=0.71521$ D as standard [14]. With $\langle 0|\mu_z|0\rangle=2.370(20)$ Debye from $|K|=3$, $J=3\rightarrow J'=4$ and with $\langle 0|\mu_z|0\rangle=2.389(20)$ D from $K=0$, $J=2\rightarrow J'=3$ we give the vibrational ground state expectation value as $\langle 0|\mu_z|0\rangle=2.38\pm0.02$ Debye.

In order to get experimental information on the dependence of the electric dipole moment on the bending of the heavy atom chain during the degenerate v_{10} bending motion, we also investigated the Stark effect of the $|K|=1$, $J=2\rightarrow J'=3$ l-type doublet in the first excited state $v_{10}=1$, $|l|=1$ [15].

The experimentally found dependence of the Stark satellites on the applied field is shown in Figure 2. As is seen from this figure the plots for the satellite frequencies belonging to the same $|M|$ values intersect for a certain M-dependent Stark-field at the center frequency of the zero field doublet, $\nu_{\text{center}}=(\nu_+ + \nu_-)/2$. From the corresponding field value $E_c(M)$ the vibrational expectation value for the dipole component in direction of the molecular symmetry axis may be calculated according to Equation (4) [15].

$$\langle v_{10}=1|\mu_{||}|v_{10}=1\rangle = \frac{hJ(J+1)(J+2)}{4E_{c(M)}KM}(\nu_+-\nu_-)\,. \tag{4}$$

Equation (4) holds as long as off-diagonal Stark-effect matrix elements which connect nondegenerate levels (i. e. levels which differ in their J and K values) may be neglected.

Since we feel that the presentation in Ref. [15] might lead to the wrong impression that further approximations need to be made which limit the applicability of Equation (4), the derivation of Eq. (4) is sketched in the Appendix. From the experimental values given in Figure 2 the Eq. (4) leads to the excited state expectation value of

$$\langle v_{10}=1|\mu_{||}|v_{10}=1\rangle = 2.36\pm0.02\,\text{D}$$

i. e. there is essentially no change with respect to the ground state expectation value.

^{14}N Hyperfinestructure

Due to the nonspherical Coulomb potential well at the position of the "prolate" ^{14}N nucleus, the latter tends to aligne itself with respect to the well. This leads to a weak coupling of nuclear spin, $\boldsymbol{I}$, and molecular rotation and causes a first order splitting of the rotational levels according to Equation (5) [16].

$$W_{\text{HFS}}=h\chi_{zz}\cdot\frac{[\frac{3}{4}C(C+1)-I(I+1)J(J+1)][3K^2-J(J+1)]}{2J(J+1)(2J-1)(2J+3)I(2I-1)}\,. \tag{5}$$

In Eq. (5) the symbols have the following meaning:

$C=F(F+1)-I(I+1)-J(J+1)$ with F, the quantum number of the overall angular momentum (including the spin of the quadrupole nucleus) ranging from $F=J-I$ to $F=J+I$ in steps of one.

$\chi_{zz}=|e|Q(\partial^2V'/\partial z^2)/h$ the quadrupole coupling constant with e the electronic charge, $Q=0.01\cdot10^{-24}\,\text{cm}^2$ [17] the nuclear quadrupole moment of the ^{14}N-nucleus and $\partial^2V'/\partial z^2$ the second derivative of the Coulomb potential in direction of the molecular axis. The prime indicates that only the Coulomb potential due to the charge distribution outside a small sphere around the nucleus enters into the expression for the quadrupole coupling constant.

From Eq. (5) and the additional F-selection rule, $\Delta F=0,\ \pm1$, it may be shown that the largest hfs-splittings of the rotational absorption lines should

occur for the $|K|=2$, $J=2 \rightarrow J'=3$ and $|K|=3$, $J=3 \rightarrow J'=4$ transitions. The splitting of the $J=2 \rightarrow J'=3$ transition is shown in Fig. 3 together with a computer simulation using the value $\chi_{zz}=+0.75$ MHz and a Lorentzian lineshape function with a halfintensity halfwidth of 50 kHz. Modulation- and wall-broadening are the dominant terms which determine this line width. Only the latter is reproduced by a Lorentzian lineshape function. Modulation broadening is responsible for the "triangle form" of the lines. The observed spectrum is extremely sensitive to minor offsets of the basis of the modulating Stark field. Due to the small quadrupole coupling constant, Stark fields on the order of 0.2 V/cm are already sufficient for effectively mixing the hyperfine states, shifting the levels, and changing the selection rules. This effect is illustrated in the computer simulations shown in Fig. 4. In the case of the $|K|=3$, $J=3 \rightarrow J'=4$ transition a higher Stark field (E on the order of 80 V/cm) is needed to separate the zero field quadrupole hyperfine spectrum from the Stark-quadrupole spectra of the nearby $|K|=1$ and $|K|=2$ lines. Since our high quality square wave generator was only capable of delivering square waves up to 10 V peak to peak, the $|K|=3$, $J=3 \rightarrow J'=4$ transition could not be used for the fit. From the observed spectrum (Fig. 3) and the experience with computer simulations using different χ_{zz} values and zero-offsets we estimate the uncertainty of the quadrupole coupling constant to be on the order of ± 0.05 MHz.

For the higher J transitions the hfs-splittings drop below the resolution power of our spectrometer. This is especially true for the transitions listed in Tab. 1, which were used for the fit of the rotational constants of the $H_3Si^{14}N^{13}CS$ species.

Discussion

The experimental results reported above may be used to get some insight into the bonding situation in silylisothiocyanate. We first discuss the bonding in terms of the two mesomer forms (II) and (III).

From the Pauling electronegativities of the elements [18] and the observed bond distances we expect dipole moments of $\mu_z=4.2$ D (Si negative) for form (II), and of $\mu_z=-14.4$ D (S negative) for form (III) (compare Figure 5). Thus the observed absolute value of $|\langle|\mu_z|\rangle|=2.38$ D might result from a 90% to 10% mixture of forms (II) and (III) leading to $\mu_z=+2.38$ D (Si negative), or from a 65% to 35% mixture leading to $\mu_z=-2.38$ D (S negative). For both choices form (II), which implies a Si = N-double bond, contributes considerably. Thus the observed dipole moment indicates that the Si-d-orbitals do considerably contribute to the occupied molecular orbitales.

The first excited state expectation value of $\langle|\mu_z|\rangle$ gives information on the dependance of μ_z on the bending motion. From the coincidence of the ground state and first excited state expectation values of μ_z

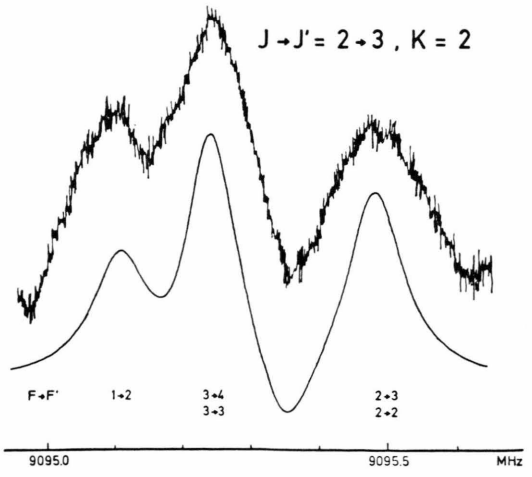

Fig. 3. Vibrational ground state hyperfine structure of the $|K|=2$, $J=2 \rightarrow J'=3$ rotational transition of the most abundant species. This hyperfine splitting was used for the determination of the quadrupole coupling constant χ_{zz}.

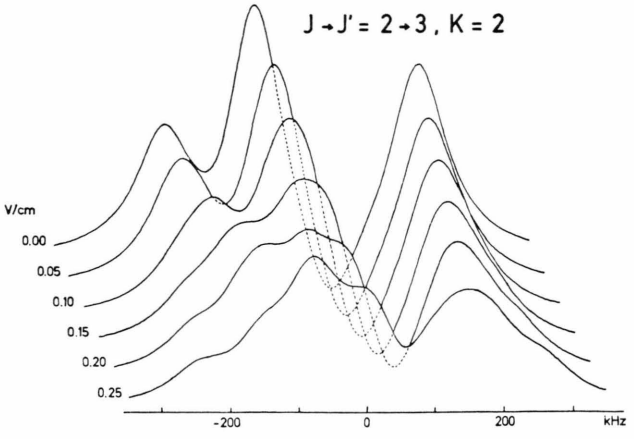

Fig. 4. Computer simulations showing the effect of a minor offset of the baseline of the modulating square wave Stark field. For the calculations the complete M_J, M_I-submatrices for the $J=2$ and $J'=3$ rotational states were diagonalized numerically and the symmetric top transition cosine matrix elements were subjected to the corresponding unitary transformation.

we conclude that μ_z remains essentially constant over the bending motion, that is up to an angle of about 20° between the SiN-bond and the CS-bond. This value follows from the observed frequency $\tilde{\nu}_{10} = 54\,cm^{-1}$ and a "reduced mass" on the order of 50 amu Å² as the square root of the harmonic oscillator expectation value for the square of the bending angle. We now turn to the bond distances. Using Pauling's covalent bond radii listed in Tab. 4 and applying a "bent bond correction" [19] of −0.02 Å for the r_{SiN} and r_{CS} distances and of −0.04 Å for the central N−C bond, the following bond distances are obtained for the limiting structures:

	r_{SiN}	r_{NC}	r_{CS}
(II) $H_3Si-N=C=S$	1.57 Å	1.21 Å	1.58 Å
(III) $H_3Si-N=C-S$	1.79 Å	1.07 Å	1.79 Å
observed values	1.673 Å	1.221 Å	1.575 Å

As is seen, the r_{NC} and r_{CS} distances are practically those predicted for a pure form (II), while the r_{SiN} distance turns out to lie between a single bond and a double bond distance. This indicates that the simple concepts upon which the above bond distance calculations are based and which work rather well for molecules containing localized orbitals only, tend to fail when applied to highly delocalized systems such as Silylisothiocyanate. However the bond distances too indicate that there is a considerable amount of double bond character and thus d-orbital contribution in the region of the Si – N-bond.

For comparison we also have calculated the dipole moment by the semiempirical quantum mechanical CNDO/2 program using the original parametrization of Pople et al. [20]. As input structure the r_s-structure shown in Fig. 1 was used. The resulting dipole moment was +0.8 D (Si negative). This value includes a +3.2 D contribution due to p-d-orbital overlap in the Si – N-region. Although the calculated CNDO value falls about 1.6 D short of the observed value, we would assume the CNDO calculation as indicative to a dipole moment with Si at the negative end of the molecule. We plan to settle the question of the direction of μ_z experimentally by a separate investigation of the molecular rotational Zeeman effect of different isotopic species [21].

Better agreement was obtained between the experimentally determined quadrupole coupling constant and the value following from the CNDO-calculation. From a simplified MO treatment in which only the atomic orbitals centred at the nitrogen nucleus are assumed to contribute appreciably, the ^{14}N quadrupole coupling constant follows as given in Eq. (6) [22]:

$$\chi_{zz} = -\left(\frac{P_{p_x,p_x} + P_{p_y,p_y}}{2} - P_{p_z p_z}\right) q_{210}(^{14}N) \,. \quad (6)$$

In Eq. (6) the value −10 MHz [23] was used for

$$q_{210}(^{14}N) = |e|\, Q \left\langle p_z \left| \frac{\partial^2 V_{coul}}{\partial z^2} \right| p_z \right\rangle / h \,.$$

P_{p_x,p_x}, P_{p_y,p_y} and $P_{p_z p_z}$ are the p_x-, p_y- and p_z-densities at the ^{14}N nucleus defined as:

$$P_{p_x,p_x} = 2 \sum_n |C_{p_x,n}|^2$$

etc. where $C_{p_x,n}$ is the coefficient of the ^{14}N-p_x atomic orbital in the n-th molecular orbital. With the CNDO-values $P^{CNDO}_{p_x,p_x} = P^{CNDO}_{p_y,p_y} = 1.295$ and $P^{CNDO}_{p_z p_z} = 1.225$ Eq. (6) predicts a ^{14}N quadrupole coupling constant of +0.70 MHz which is in good agreement with the observed value of +0.75 MHz.

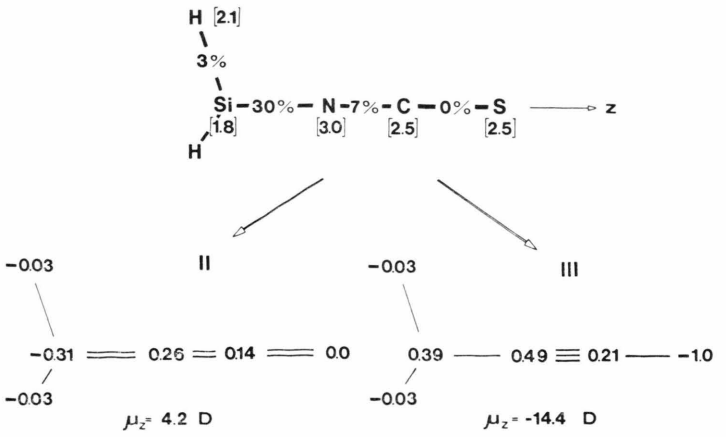

Fig. 5. Pauling electronegativities (in bracketts) and ionic character (in %) of each covalent bond are given in the first row. The second row shows the resulting Pauling atomic charges, Q_n (in units of $|e|$) for the two mesomer forms II and III. Also given are the corresponding electric dipole moments, calculated with the structure shown in Fig. 1 according to $\mu_z = \sum_n^{atoms} Q_n \cdot |e| \cdot z_n$.

It is interesting to compare the ^{14}N quadrupole coupling constant observed here with the one observed for the quasi-symmetric top SiH_3NCO ($\chi_{zz} = +1.8$ MHz [24]). This comparison indicates, that the population of the nitrogen p_x and p_y orbitals is smaller for SiH_3NCS. The greater stability of the linear configuration in SiH_3NCS as compared to SiH_3NCO can thus be "explained" by a stronger delocalization of the p_x and p_y orbitals.

Appendix:

The Stark Effect of the *l*-type Doublets

For the discussion of the Stark-effect of the *l*-doublets we neglect all other vibrations except the degenerate ν_{10} bending motion. Within this simplified model the Eigenfunctions of the vibrational Hamiltonian which correspond to the *l*-type doublets may be approximated by the symmetrized products of a symmetric top Eigenfunction with an Eigenfunction of the two-dimensional harmonic oscillator [25] as given in Eq. (A.1):

$$\Psi_{\pm}(\alpha,\beta,\gamma,r,\varphi) = \frac{1}{\sqrt{2}}\left[\Psi_{J,K=1,M}(\alpha,\beta,\gamma)\right. \tag{A.1}$$
$$\left.\cdot\,\Phi_{v,l=1}(r,\varphi) \pm \Psi_{J,K=-1,M}(\alpha,\beta,\gamma)\Phi_{v,l=-1}(r,\varphi)\right]$$

$\Psi_{J,K,M}(\alpha,\beta,\gamma)$ = symmetric top Eigenfunction with α, β, γ the Eulerian angles describing the orientation of the molecular coordinate system with respect to the space fixed Laboratory frame.

$\Phi_{v,l}(r,\varphi)$ = harmonic oscillator Eigenfunction with $r^2 = Q_{10x}^2 + Q_{10y}^2$ and $\tan\varphi = Q_{10y}/Q_{10x}$. Q_{10x} and Q_{10y} are the normal coordinates corresponding to the degenerate bending modes in x- and y-direction perpendicular to the molecular z-axis.

Within this basis, the 2 by 2 Hamiltonian submatrices corresponding to the Ψ_+-, Ψ_--functions of Eq. (A.1) are diagonal, with a splitting of the diagonal elements given by $\pm(q/4)(v+1)J(J+1)h$ [26]. In H_3SiNCS the "*l*-type doubling constant" q has the value 2.783 MHz.

If the exterior Stark-field is switched on, the space degeneracy (M-degeneracy) is lifted due to the operator corresponding to the potential energy of the molecular electric dipole moment in the exterior field:

$$V_{\text{pot}} = -\boldsymbol{\mu}\cdot\boldsymbol{E} \tag{A.2}$$
$$= -\left[\left(\mu_{0z} + \tilde{\tilde{\mu}}_z\left(Q_{10x}^2 + Q_{10y}^2\right) + \ldots\right)\cos z\,Z\right.$$
$$\left. + \left(\tilde{\mu}_x Q_{10x} + \ldots\right)\cos x\,Z + \left(\tilde{\mu}_y Q_{10y} + \ldots\right)\cos y\,Z\right] E\,.$$

On the right hand side μ is expanded with respect to the normal coordinates taking account of the cylindrical symmetry about the molecular axis. $\cos x\,Z$ etc. are the direction cosines between the molecular axes and the space fixed Z-axis which is determined by the direction of the exterior field. E is the electric field strength. From V_{pot} only the first term involving $\cos z\,Z$ leads to matrix elements which connect the closely degenerate *l*-doublet levels ($\cos x\,Z$ and $\cos y\,Z$ only connect states which differ in K by ± 1):

$$\langle\Psi_+|V_{\text{pot}}|\Psi_-\rangle =$$
$$-\langle\Psi_+|\left(\mu_{0z} + \tilde{\tilde{\mu}}_z r^2 + \ldots\right)\cos z\,Z\,E\,|\Psi_-\rangle$$
$$= -\frac{E}{2}\langle\Psi_{J,K=1,M}\Phi_{v,l=1} + \Psi_{J,K=-1}\Phi_{v,l=-1}|$$
$$\cdot\left|\mu_{0z}\cos z\,Z + \tilde{\tilde{\mu}}_z\cos z\,Z\,r^2 + \ldots\right|\Psi_{J,K=1,M}\Phi_{v,l=1}$$
$$-\Psi_{J,K=-1,M}\Phi_{v,l=-1}\rangle \tag{A.3a}$$

$$= -\frac{\mu_{0z}E}{2}\left\{\langle\Psi_{J,K=1,M}|\cos z\,Z|\Psi_{J,K=1,M}\rangle\right.$$
$$\left.-\langle\Psi_{J,K=-1,M}|\cos z\,Z|\Psi_{J,K=-1,M}\rangle\right\}$$
$$-\frac{\tilde{\tilde{\mu}}_z E}{2}\left\{\langle\Psi_{J,K=1,M}|\cos z\,Z|\Psi_{J,K=1,M}\rangle\right.$$
$$\cdot\langle\Phi_{v,l=1}|r^2|\Phi_{v,l=1}\rangle - \langle\Psi_{J,K=-1,M}|\cos z\,Z$$
$$\left.\cdot\,|\Psi_{J,K=-1,M}\rangle\langle\Phi_{v,l=-1}|r^2|\Phi_{v,l=-1}\rangle\right\} \tag{A.3b}$$

$$= -\frac{EM}{J(J+1)}\left[\mu_{0z} + \tilde{\tilde{\mu}}_z\langle\Phi_{v,l=1}|r^2|\Phi_{v,l=1}\rangle\right];$$
$$\text{for } K = \pm 1\,. \tag{A.3c}$$

In the step from (A.3a) to (A.3b) it is used that the matrix elements of $\cos z\,Z$ are diagonal in K with $\langle\Psi_{J,K,M}|\cos z\,Z|\Psi_{J,K,M}\rangle = [KM/J(J+1)]$. In the step from (A.3b) to (A.3c) it is used that the r-dependence of the harmonic oscillator wave functions is the same for both *l*-values i. e.

$$\langle\Phi_{v,l}|r^2|\Phi_{v,l}\rangle = \langle\Phi_{v,-l}|r^2|\Phi_{v,-l}\rangle.$$

We further note that the diagonal elements due to the Stark-perturbation vanish, i. e.

$$\langle\Psi_+|V_{\text{pot}}|\Psi_+\rangle = \langle\Psi_-|V_{\text{pot}}|\Psi_-\rangle = 0$$

because we are using the symmetrized wavefunctions given in Eq. (A.1). Thus in the presence of the Stark field the 2 by 2 matrices corresponding to the *l*-doublets take the form:

$$\begin{pmatrix} \overline{W}_{J,|K|,v} + h\frac{q}{2}J(J+1) & -\frac{\langle|\mu_z|\rangle ME}{J(J+1)} \\ -\frac{\langle|\mu_z|\rangle ME}{J(J+1)} & \overline{W}_{J,|K|,v} - h\frac{q}{2}J(J+1) \end{pmatrix}$$

Here $\overline{W}_{J,|K|,v}$ is the average energy of the l-doublet levels in the absence of the field. At low Stark-fields with E only few V/cm one may neglect all other off diagonal Stark-effect matrix elements, since they connect widely spaced energy levels (typically on the order of several GHz).

Within this approximation the presence of the Stark-field leads to the following expressions for the energy levels, which are given by the Eigenvalues of the 2 by 2 matrices above:

$$W_{+} = \overline{W}_{J,|K|=1,v_{10}=1} + \sqrt{\left(\frac{q}{2} J(J+1)\right)^2 + \left(\frac{\langle|\mu|\rangle E M}{J(J+1)}\right)^2},$$
$$W_{-} = \overline{W}_{J,|K|=1,v_{10}=1} - \sqrt{\left(\frac{q}{2} J(J+1)\right)^2 + \left(\frac{\langle|\mu|\rangle E M}{J(J+1)}\right)^2}. \quad \text{(A.4)}$$

Figure A.1 shows the corresponding field dependence of the l-doublet levels involved in the $J=2 \rightarrow J'=3$, $|K|=1$, $|l_{10}|=1$, $v_{10}=1$ rotational transition of H_3SiNCS. Taking into account the microwave transition selection rules ($\boldsymbol{E}_{\text{microwave}}$ parallel $\boldsymbol{E}_{\text{Stark}}$) which follow from the dipole matrixelements within the basis given by Equations (A.1), the crossing of the Stark satellite frequencies with equal $|M|$ occurs at the frequency

$$\nu_0 = (\overline{W}_{J+1,|K|,v} - \overline{W}_{J,|K|,v})/h$$

and the corresponding Stark field, $E_{C(M)}$ follows from the condition given in Eq. (A.5)

$$\left[h\frac{q}{2}(J+1)(J+2)\right]^2 + \left[\frac{\langle|\mu_z|\rangle E_{C(M)} M}{(J+1)(J+2)}\right]^2 \overset{!}{=} \left[h\frac{q}{2}J(J+1)\right]^2 + \left[\frac{\langle|\mu_z|\rangle E_{C(M)} M}{J(J+1)}\right]^2. \quad \text{(A.5)}$$

Due to the favourable J-dependence of the q- and $\langle|\mu_z|\rangle$-contributions, the square root may be drawn after rearranging. This leads to Eq. (A.6). With $E_{C(M)}$ the Stark-field at the crossing point:

$$\frac{q}{2}(J+1) \overset{!}{=} \frac{\langle|\mu_z|\rangle M E_{C(M)}}{h J(J+1)(J+2)}. \quad \text{(A.6)}$$

Since the zero field splitting between the l-doublet frequencies is given by $\Delta\nu_0 = 2q(J+1)$ (compare Fig. A.1) we may express q in Eq. (A.6) by $\Delta\nu_0 = |\nu_+ - \nu_-|$ which leads to the final expression. Eq. (A.7) used to determine the expectation value $\langle v_{10}=1, l=1 \,|\, \mu_z \,|\, v_{10}=1, l=1\rangle$ in the first excited state of the bending motion.

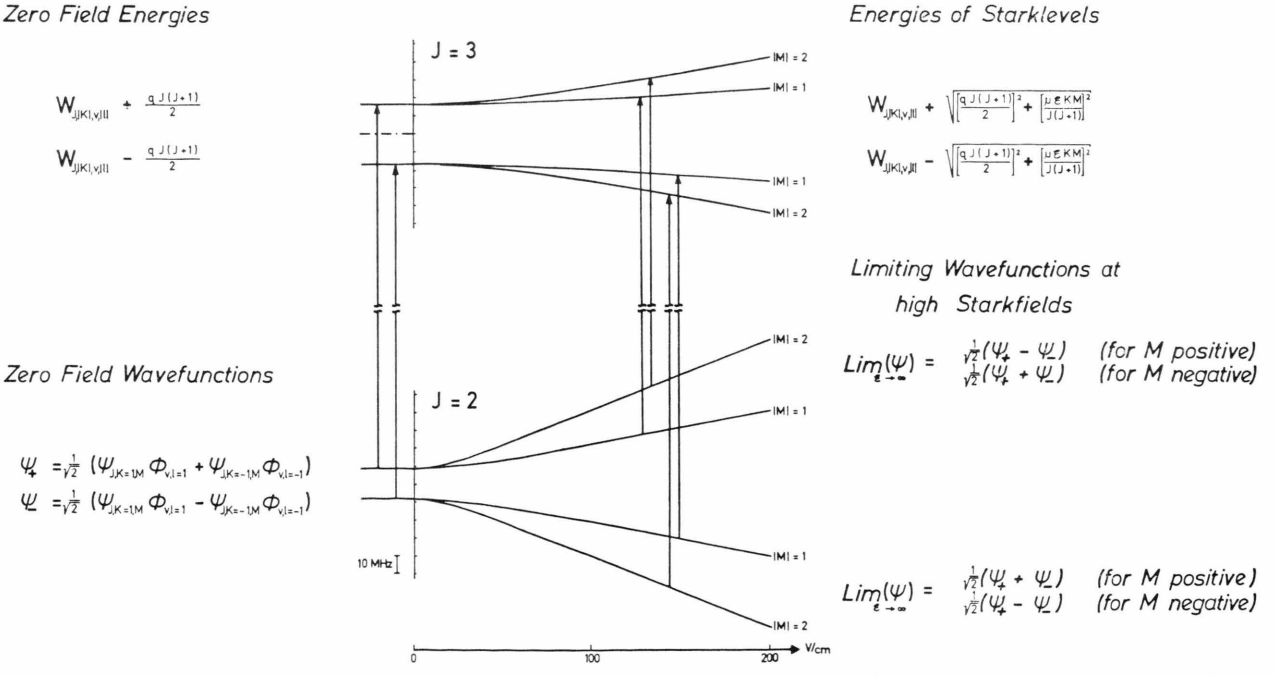

Fig. A1. To scale drawing of the field dependence of the M_J-sublevels for the $|K|=1$, $J=2 \rightarrow J'=3$ l-doublet in H_3SiNCS. Also given are the energy expressions and wavefunctions for the limiting cases. (The electric dipole moment is assumed to point in the direction of the molecular axis.) $\overline{W}_{J,|K|,v,|l|}$ stands for the average energy of the corresponding zero field doublet.

$$\langle v_{10}=1, l=1 \mid \mu_z \mid v_{10}=1, l=1\rangle = \frac{\Delta\nu_0 h J(J+1)(J+2)}{4 M E_{c(M)}} . \quad \text{(A.7)}$$

At higher Stark-fields such as used in the present work, the second order contributions, although still minor corrections, are no more negligible in the expressions for the energy levels. However they are practically identical for sublevels corresponding to the same $|M|$ values (equal matrix elements). Thus they drop out in the "crossing condition", leaving the original expression Eq. (A.7) unaltered.

[1] E. A. V. Ebsworth, R. Mould, R. Taylor, G. R. Wilkinson, and L. A. Woodward, Trans. Farad. Soc. **58,** 1069 [1962].
[2] D. R. Jenkins, R. Kewley, and T. M. Sugden, Trans. Farad. Soc. **58,** 1284 [1962].
[3] R. Kewley, K. V. L. N. Sastry, and M. Winnewisser, J. Mol. Spectr. **10,** 418 [1963].
[4] a) J. Kraitchman, Am. J. Phys. **21,** 17 [1953]; b) C. C. Costain, J. Chem. Phys. **29,** 864 [1958].
[5] J. Pople and D. Beveridge, Approximate molecular orbital theory, McGraw-Hill, New York 1970.
[6] R. H. Hughes and E. B. Wilson, Jr, Phys. Rev. **72,** 1265 [1946].
[7] H. D. Rudolph, Z. Angew. Phys. **13,** 401 [1961].
[8] U. Andresen and H. Dreizler, Z. Angew. Phys. **30,** 207 [1970].
[9] F. Mönig, Diplom-Thesis, Freiburg 1963, p. 50—55; H. J. Tobler, A. Bauder, and Hs. H. Günthard, J. Sci. Instr. **42,** 236 [1965]; H. J. Tobler, H. U. Wemgler, A. Bauder, and Hs. H. Günthard, loc. cit. **42,** 240 [1965].
[10] R. Schwarz, Thesis, Kiel 1974.
[11] Z. F. Slawsky and D. M. Dennison, J. Chem. Phys. **7,** 509 [1939].
[12] K. F. Dössel and A. G. Robiette (Part I in this series).
[13] Ref. 4 b Equation (3).
[14] J. S. Muenther, J. Chem. Phys. **48,** 4544 [1968].
[15] W. Gordy and R. L. Cook, Microwave molecular spectra, Interscience Publishers, John Wiley, New York 1970, Sec. 10.5.
[16] C. H. Townes and A. L. Schawlow, Microwave spectroscopy, McGraw-Hill Book Company, New York 1955, Sec. 6.3.
[17] Ref. [15] Appendix V.
[18] L. Pauling, The Nature of the Chemical Bond, Cornell University Press, New York 1960, Sec. 3.9.
[19] Ref. [18], Sec. 7.
[20] Ref. [5].
[21] R. F. Schwarz, Phys. Rev. **86,** 606 [1900]; Am. Thesis, Harvard University (1952); D. H. Sutter and W. H. Flygare, The Molecular Zeeman Effect in Topics in Current Chemistry, Vol. 63, Sec. II.B.
[22] Ref. [15], Sec. 14.5.
[23] Ref. [15], p. 594.
[24] J. A. Duckett, A. G. Robiette, and I. M. Mills, J. Mol. Spectr. **62,** 34 [1976].
[25] For the symmetric top wavefunctions and direction cosine matrix elements c. f. Ref. [11], Sec. 2.5 and Sec. 2.6. For the twodimensional harmonic oscillator c. f. L. Pauling and E. B. Wilson jr., Introduction to quantum mechanics, McGraw-Hill, New York 1935, Sec. IV-17.
[26] For the definition of q c. f. the review article on l-type doubling by T. Oka, J. Chem. Phys. **47,** 5410 [1967].